OPTIMIZED ENERGY CONSUMPTION MODEL FOR SMART HOME USING IMPROVED DIFFERENTIAL EVOLUTION ALGORITHM

ABSTRACT

This paper proposes an improved enhanced differential evolution algorithm for implementing demand response between aggregator and consumer. The proposed algorithm utilizes a secondary population archive, which contains unfit solutions that are discarded by the primary archive of the earlier proposed enhanced differential evolution algorithm. The secondary archive initializes, mutates and recombines candidates in order to improve their fitness and then passes them back to the primary archive for possible selection. The capability of this proposed algorithm is confirmed by comparing its performance with three other well-performing evolutionary algorithms: enhanced differential evolution, multiobjective evolutionary algorithm based on dominance and decomposition, and non-dominated sorting genetic algorithm III. This is achieved by testing the algorithms' ability to optimize a multi-objective optimization problem representing a smart home with demand response aggregator. Shiftable and non-shiftable loads are considered for the smart home which model energy usage profile for a typical household in Johannesburg, South Africa. In this study, renewable sources include battery bank and rooftop photovoltaic panels. Simulation results show that the proposed algorithm is able to optimize energy usage by balancing load scheduling and contribution of renewable sources, while maximizing user comfort and minimizing peak-to-average ratio.

Keywords: HEMS, evolutionary algorithms, RES, optimization, demand response

1 INTRODUCTION

A smart grid (SG) is a power system that is capable of efficiently allocating electricity based on information received from intelligent technologies (hardware and software) deployed within the system [1]. From the consumer perspective, a curtailment of energy usage pattern in return for financial incentives has led to the development of home energy management systems. The idea of home energy management system began in 1979 with the use of a microprocessor-based algorithm for solar energy management [2]. This system was developed to provide a standardized platform for incorporating various solar energy storage and management systems that had previously existed. The system comprised mode selection and prioritization which determined the application of the energy from the solar panel system. The idea was to control priority between pumps, valves and a fan depending on whether heating or cooling was required. Control of the different modes of heating and cooling for a household using solar energy was achieved using a system initialization panel (SIP). The controlled sequence for the valves, pumps and fan was specified in a relay table. In current HEMS, energy management using demand response (DR) has been made possible using computer algorithms which are capable of communicating between energy distribution companies and end users. This approach has made it possible for consumers to prioritize energy usage in terms of both period and duration of use. In this way, the energy utility gains through eliminating the need for untimely grid expansions, while the consumers receive financial incentives.

Residential demand response programs involve the use of knowledge of real-time energy trading to determine the pattern of energy usage. The motivation for such programs can be either price- or incentive-based [3]. This strategy is similar to that used by commodities traders to profit from selling such commodities based on knowledge of the price trends. In other words, advancements in computing and smart energy devices have made it possible for electricity to be considered as a commodity. An efficient demand response strategy effectively balances cost savings with consumer energy usage pattern [1]. Demand response involves two-way communication between consumers and utility companies, which results in a much better utilization of electricity. Demand response is an effective strategy for managing energy resources of the existing grid as opposed to expansion of the grid in order to accommodate ever-increasing energy demands. With demand response, loads that are shiftable (schedulable) can be used during off-peak periods when energy prices are comparatively lower. Optimal demand response is achieved using load forecasting [4]-[9], energy price forecasting [10]-[11] as well as the injection of renewable energy sources [12]-[18].

There are a number of intelligent algorithms that have been employed in both the control and scheduling of devices in home energy management systems. Some of the most widely used strategies include artificial neural networks (ANNs), fuzzy logic controllers (FLCs) and adaptive neuro-fuzzy inference system (ANFIS) [3]. With regard to evolutionary algorithms, differential evolution (DE) has been used to successfully implement load scheduling [19]-[20]. Scheduling has been done based on consideration of consumer comfort, amount paid per unit of energy (with demand side management) and time delay reduction [20]-[24]. In this paper, the level of consumer comfort is determined according to the duration and period for which schedulable appliances remain inactive for the purpose of maximizing financial incentives from demand response programs. As an example, a consumer may have to sacrifice some level of comfort by shifting operation of a washing machine from morning hours to other off-peak periods within the day. Evolutionary algorithms are generally population-based. This means that they can be used to find optimal solutions to complex problems. With regard to use of differential evolution algorithm for demand response, the enhanced DE algorithm (EDE) has yielded promising results in recent literature [19]-[20], [25].

Contribution

The aim of this paper is to present an improved enhanced DE algorithm (*i*EDE). *i*EDE uses a two-archive approach for the mutation and recombination of unfit candidates among the population. *i*EDE is to be deployed by demand response aggregator with renewable energy sources in order to maximize consumer comfort and energy savings for demand response program. The performance of *i*EDE is compared with three other evolutionary algorithms: enhanced differential evolution, multi-objective evolutionary algorithm based on dominance and decomposition (MOEA/DD) and non-dominated sorting genetic algorithm III (NSGAIII). The constructed objective function (OF) minimizes the daily cost of energy while minimizing peak-to-average ratio (PAR) and waiting time delay. The rest of the paper is organized as follows: Section 2 reviews the use of population-based heuristic algorithms for demand response. Section 3 details the proposed approach for improving the EDE algorithm for deployment in demand response aggregator. Section 4 discusses the proposed two-archive approach for improving performance of the enhanced differential evolution algorithm. Section 5 presents and discusses simulation results comparing performance of the improved EDE with the three other specified algorithms. Section 6 concludes the paper.

2 IMPLEMENTATION OF DEMAND SIDE MANAGEMENT STRATEGIES USING HEURISTIC ALGORITHMS

Population-based algorithms are problem-solvers which use a predetermined number of search agents (commonly called particles) to find the optimal solution to a problem. Such problems are formulated as an objective function with specified parameters and constraints. Population-based algorithms are effective for solving computationally complex problems because their search strategy is generally non-deterministic or heuristic. Therefore, they use a randomized approach to obtain the optimal solution(s) to a given problem. Examples of population-based algorithms include evolutionary and swarm algorithms [26]-[28]. With regard to smart grids, population-based algorithms have been applied to network communications [29] and demand side management [25], [30]-[31]. Demand side management (DSM) involves a number of strategies to maintain electricity supply to consumers with existing infrastructure in spite of ever-increasing demand [1]. DSM involves two key aspects: demand response and energy efficiency. Demand response (DR) is defined as a process of curtailing electricity demand to match supply [1]. One common approach to achieving this is for utility companies to pay consumers to reduce or reschedule energy consumption. Since demand side management involves use of fixed electricity supply to meet growing energy needs of consumers, this paper proposes the use of an improved enhanced differential evolution algorithm to implement demand response for a home energy management system. Differential evolution (DE) is an evolutionary algorithm which has been used to optimize demand side management for home management systems with promising results. This section details some of the applications of evolutionary algorithms in reducing energy costs and improving consumer comfort.

In [4], a shark smell optimization algorithm (SSO) was used to optimize the performance of Elman neural network (ENN). This architecture was used to optimize over-fitting/under-fitting of the neural network which enhanced electricity load forecasting capability of the ENN. SSO is a population-based strategy which is inspired by the approach taken by a shark to locate its prey. The location of prey is called the optimal point, while the shark updates its position with respect to the optimal point. This proposed strategy outperformed the back propagation neural network (BPNN) and radial basis function neural network (RBFNN) with respect to reduction of root mean square error (RMSE) and mean absolute percentage error (MAPE). A similar approach was used in [12] to improve the prediction accuracy of solar irradiation for a case study area located in Oregon, USA. The proposed SSO and neural network combination also outperformed six other neural network structures in 24 test functions.

A genetic algorithm (GA) for optimal load scheduling considering day-ahead electricity pricing was presented in [7]. The proposed algorithm considered load scheduling for three categories of residential consumers. Two fitness functions were used in the simulations: one prioritized cost (with cheapest strategy being the best), while the other considered consumer comfort. 90%

of consumer needs being fulfilled was considered to be satisfactory. Single-point crossover was used with 1,000 generations. From simulation results, energy cost savings for the three categories of consumers was 17.8%, 14% and 14% respectively compared to a scenario in which no GA was used. In [17], an artificial immune algorithm (AIA) was used to solve a multi-objective optimization problem (MOP). The MOP consisted of 3 objectives relating to the grid utility, DR aggregator and customers respectively. The grid utility aimed at minimizing operation cost while giving part of the savings back to the DR aggregator; the DR aggregator sought to minimize grid power contributions by maximizing distributed generation from conventional generators and renewable energy sources. The customers desired to optimize tradeoff between comfort and energy savings. The proposed demand side management (DSM) optimization model was applied to a utility in the United Kingdom. The AIA model saved the utility £5,684 in generation costs, while the peak-to-average ratio (PAR) was reduced by 5.33%. Also, the DR aggregator earned £12,632 in profit while saving the consumers £620 in electricity bill for a single day. Benefits of population-based metaheurisitic algorithms in DSM can also be seen in [32]-[46].

Differential evolution (DE) is a population-based metaheurisitic evolutionary algorithm which has been used extensively to improve DSM in smart grids. In particular, the work done in [19] proposed an enhanced DE (EDE) algorithm which adaptively tuned the crossover rate, scaling factor and population size using five trial vectors. The aim was to improve the fitness of the final solution set by selecting the best possible set of candidates to constitute the initial population. The parameters considered were PAR, total cost of electricity, user comfort and energy consumption pattern. Simulation results showed that EDE reduced both electricity bill and PAR compared to conventional DE. EDE was also used to obtain an improved load profile for a HEMS in [20].

This paper proposes an improved EDE by considering two population archives for optimizing the solution space. The idea behind the two-archive approach is to reuse previously unfit solutions in cases of premature convergence or loss of selection pressure.

3 PROPOSED METHODOLOGY

This methodology section is divided into three sub-sections. The first sub-section specifies the configuration of the aggregator-smart home system. The objective minimization function with parameter and constraint specification is discussed next, and then the strategy for peak-to-average ratio and electricity cost reduction using proposed two-archive EDE is presented.

3.1 Two-layer aggregator-smart home system

Demand response aggregators combine a number of consumers (often called a cluster) in order to represent a significant proportion of the localized electricity demand sector [17]. They act as intermediaries between consumers and the electricity supply utility. This role is similar to that of a sales representative who is a middleman between customers and the product/service company. Therefore, the role of the demand response aggregator is two-fold:

- It provides consumer energy usage information to the utility that would enable the utility to cut electricity supply costs to a minimum. This in turn minimizes wear and tear on electricity supply equipment, and maximizes the bonus that the DR aggregator receives from the utility company

- The DR strategy employed by the aggregator (based on time-of-use (ToU) and appliance scheduling habits of consumer) is used to reduce the amount paid for electricity. This acts as an incentive to the consumers to be actively involved in DR programs

This dual role of the DR aggregator is likely to become more commonplace as smart grid concept improves and evolves. Since it is difficult for utility companies to be directly linked to the final consumer, the role that demand response aggregators play is very significant. It is likely that demand response aggregators will become a point of synergy for both utility companies and consumers as they seek to improve energy usage efficiency, maximize benefits and minimize losses. This paper will focus on the objectives, parameters and constraints that exist between the DR aggregator and the final consumer only (excluding those that exist between the utility and DR aggregator). An illustration of the relationship between the DR aggregator and consumers is given in Fig. 1. In this paper, a single consumer home is being considered with demand response aggregator. In a real-time aggregator, other consumers can be considered based on their energy usage patterns and requirements.

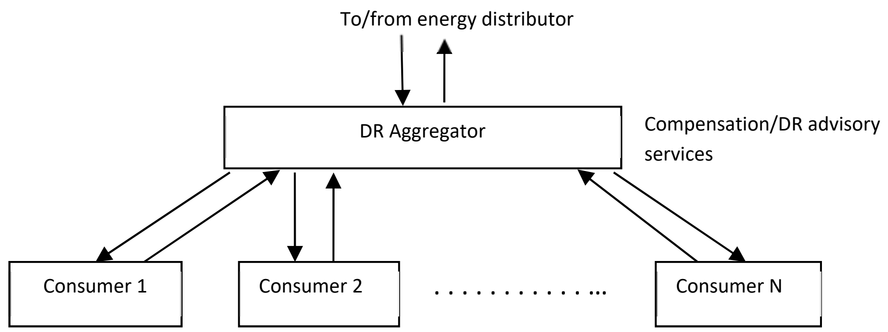

Fig. 1 Demand response Aggregator connected to cluster of consumers

With respect to the demand response aggregator, there is a compensation function which is used to reward consumers who participate in demand side management programs. According to [47], this function is represented as:

$$\Gamma(t) = \sum_{t=1}^{T}((-\gamma(\theta_t - \eta_t)^2 + \delta)) \quad (1)$$

$\Gamma(t)$ is the compensation function, γ and δ are compensation coefficients, θ_t is energy consumption vector of aggregated consumers, η_t represents the vector of projected generation.

The demand response aggregator has an objective of maximizing its net payoff from the distribution utility [16]. In this paper, this objective has been modified to include a renewable energy source (RES) utilization coefficient, C_{res} defined as:

$$C_{res}(i) = \sum_{i=1}^{n} x_i \quad (2)$$

x_i is the contribution from RES i. $C_{res}(i)$ represents the hourly contribution of each renewable energy source utilized in the home energy management system. For this paper, the renewable sources include battery bank and rooftop solar panel (i.e. $n = 2$). C_{res} is obtained by the ratio of the hourly contribution (in terms of real power) of RES i to the daily energy consumption of the consumer.

In general, the RES utilization coefficient can be specified for each consumer in the cluster such that:

$$C_{con,i} = \mu C_{res} : 0 \leq \mu \leq 1 \quad (3)$$

$C_{con,i}$ is the total contribution of renewable energy sources utilized by consumer i. This coefficient contributes to improving overall compensation to the demand response aggregator from the energy distribution utility, and consequently, financial reward to the consumers in the cluster. μ is a weighting factor whose value increases as the number of renewable energy sources utilized by consumer i increases. This would increase compensation to consumers as they increase usage of renewable sources as part of their demand response strategy. μ is determined as a ratio of real power generated from renewable sources to the real power requirement of the smart home being considered.

Therefore, with regard to the compensation function of demand response aggregator from distribution utility, Equation (1) is modified as:

$$\Gamma(\mathrm{t}) = \sum_{t=1}^{T}\left(\left(\left(-\gamma(\theta_t - \eta_t)^2 + \delta\right)\right) - C_{res}(i)\right) \quad (4)$$

The appliance schedule for the proposed smart home is shown in Table 1. The HEMS consists of smart plugs and devices which are Zigbee enabled. Therefore, they can share energy usage information wirelessly with the HEMS. The smart home is configured to meet the daily energy needs for two adults in a standard apartment in Johannesburg, South Africa. The apartment consists of one living room, one kitchen, one bathroom/toilet, and one bedroom. Assumed daily energy usage is based on energy usage profiles for one weekday and one weekend day each for summer and winter seasons respectively. Average daily temperatures for summer and winter in Johannesburg are obtained from [48]. The temperature variation across the year for the city of Johannesburg is shown in Fig. 2. It is assumed that both adults are working class individuals with jobs from 9:00 am to 5:00 pm from Monday to Friday. It is assumed that both adults stay at home on weekends.

Table 1 Appliance Schedule for Apartment

Appliance	Rating (KW)	Number	Operating time (hr)	Schedule	Energy usage sharing
Geyser	3.5	1	06:00-07:00, 19:00-20:00	Shiftable	Smart plug
Electric kettle	2.0	1	07:00-09:00	Shiftable	Smart plug
Toaster	1.5	1	07:00-08:00	Shiftable	Smart plug

Microwave oven	1.0	1	18:00-20:00	Shiftable	Smart plug
Dishwasher	1.0	1	08:00-09:00, 21:00-22:00	Shiftable	Smart plug
Vacuum cleaner	1.7	1	21:00-23:00	Shiftable	Smart plug
Electric iron	1.2	1	06:00-07:00, 22:00-23:00	Shiftable	Smart plug
Washing machine	0.33	1	22:00-00:00	Shiftable	Smart plug
TV	0.065	1	07:00-09:00, 18:00-23:00	Shiftable	Smart plug
Pool heater*	2.5	1	20:00-22:00	shiftable	Smart plug
Electric stove/oven	4.0	1	07:00-08:00, 18:00-20:00	Shiftable	Smart plug
AC*	3.0	1	18:00-22:00	Shiftable	Smart plug
Refrigerator	0.25	1	00:00-00:00	Non-shiftable	Smart plug
Lights*	0.024	10	06:00-08:00, 18:00-23:00	Shiftable	Zigbee enabled
Bedroom heater*	0.8	1	23:00-06:00	Shiftable	Smart plug
Miscellaneous loads	1.0	-	07:00-09:00, 18:00-23:00	Shiftable	Smart plug

*With respect to the pool heater, it is used between 20:00-22:00 during winter, and 20:00-21:00 in summer. The AC is used between 18:00-22:00 during summer only. It is not used in winter. The lights are switched on from 17:00-23:00 on winter days because of shorter days and longer nights. The bedroom heater is used between 23:00-06:00 during winter only. It is not used in summer.

Fig. 3 shows the variation in unit price of electricity (cents/KWh) based on ToU charges for the city of Johannesburg during weekdays and weekend days. For weekdays, off-peak hours

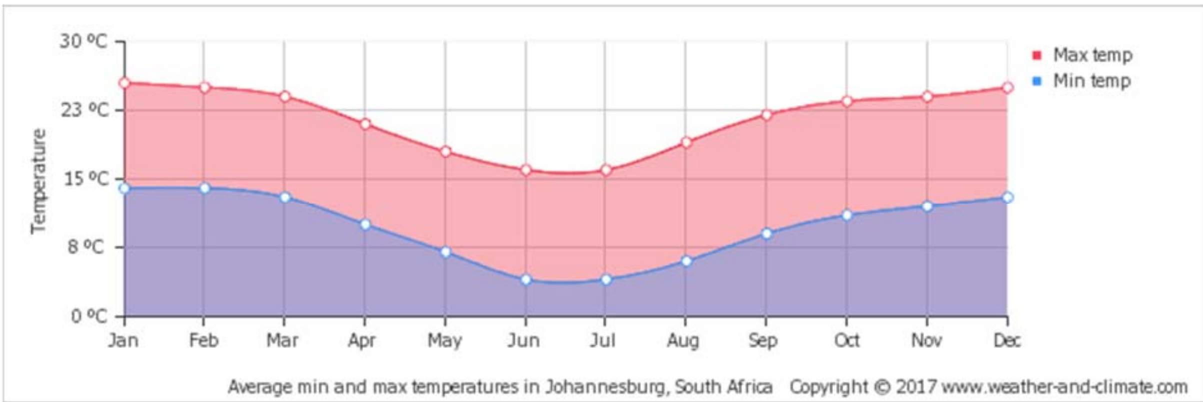

Fig. 2 Average monthly temperature for Johannesburg [47]

are between 22:00-06:00, peak hours between 10:00-12:00 and 20:00-22:00. Standard rates apply between 09:00-10:00 and 12:00-19:00. For weekend days, only standard and off-peak rates apply [48]. The unit rate variation is the same during winter. The only difference is that there is an increase of 58%, 17% and 7% respectively for peak, standard and off-peak periods respectively [48].

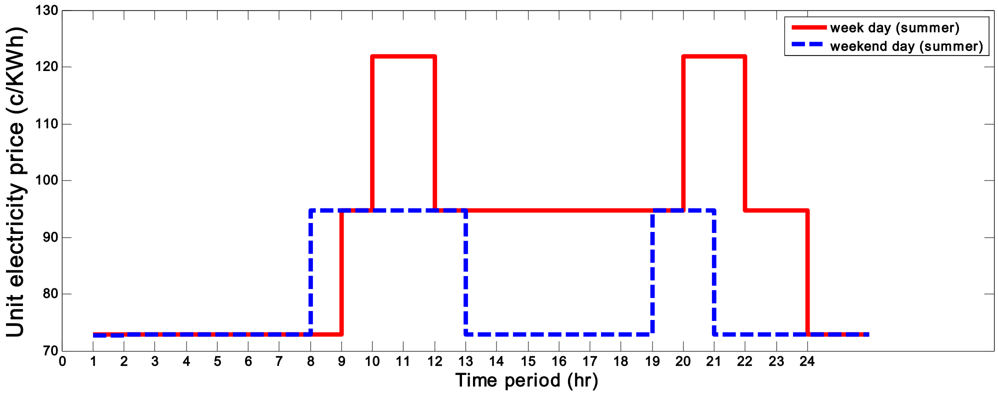

Fig. 3 Unit electricity Price Variation over 24 hours for Johannesburg based on ToU [49]

3.2 Objective Minimization Function with Parameter and Constraint Specification

The conceptual smart home uses a solar photovoltaic (PV) panel and a battery as alternative energy sources. According to [49], power supplied by solar panel is given by the product of terminal voltage and output current (Note: In all equations, (·) represents 'product'):

$$P_{solar} = V_{T,solar} \cdot I_{out,solar} \tag{5}$$

From Equation (5):

$$V_{T,solar} = \frac{n_s k T_{irr}}{e_c} \tag{6}$$

$V_{T,solar}$ is the solar thermal voltage of the PV panel, $I_{out,solar}$ is output current of PV panel, n_s is the number of cascaded cells in the PV panel, k is Boltzmann constant, T_{irr} is irradiated temperature of PV panel, e_c is electronic charge supplied by PV panel.

$$I_{out,solar} = I_{irr} - I_{dsat}\left(e^{\left(\frac{V_{out}+I_S R_S}{Q_{fd} V_{T,solar}}\right)} - 1\right) - \left(\frac{V_{out}+I_S R_S}{R_{par}}\right) \tag{7}$$

I_{irr} is the irradiated current, I_{dsat} is the diode saturation current, V_{out} is the output voltage of PV module, I_s is series current of solar cell, R_s is series resistance of solar cell, Q_{fd} is diode quality factor, $V_{T,solar}$ is solar thermal voltage, R_{par} is parallel resistance of solar cell.

The battery parameters are with respect to the state-of-charge (SoC) for charging and discharging. According to [51], state-of-charge for the battery can be represented as:

$$\varphi_{t+1} = \frac{\varphi_t + \vartheta_c \cdot P_{c,t} \cdot \partial t_c}{\epsilon_c} - \frac{P_{d,t} \cdot \partial t_d}{\vartheta_d \cdot \epsilon_c} - \varsigma \cdot \partial t_{sd} \tag{8}$$

φ_{t+1} is the SoC of battery (lead acid or Li-ion) at the next time step, φ_t is battery SoC at present time step (Note: Each time step is represented by 1 hour), ϑ_c is the battery charging efficiency,

$P_{c,t}$ is battery charging power, ∂t_c is charging time step, ϵ_c is charging rate of battery, $P_{d,t}$ is battery discharging power, ∂t_d is discharging time step, ϑ_d is the battery discharging efficiency, ς is self-discharge rate of battery, ∂t_{sd} is the self-discharging time step.

The battery is prevented from overcharging or over-discharging based on Equations (9) and (10) respectively [51]:

$$0 \leq P_{c,t} \leq P_{c,t,max} \cdot \omega_{c,t} \quad (9)$$

$$0 \leq P_{d,t} \leq P_{d,t,max} \cdot \omega_{d,t} \quad (10)$$

$P_{c,t,max}$ is the maximum allowed charging power level of the battery (set to 90% of rated battery power), $\omega_{c,t}$ indicates the battery charging status. If $\omega_{c,t} = 1$, then the battery is charging. Else, it is discharging, $P_{d,t,max}$ is the minimum allowed discharging power level of the battery (set to 30% of rated battery power), $\omega_{d,t}$ indicates the battery discharging status. If $\omega_{d,t} = 1$, then the battery is discharging. Else it is charging. $P_{c,t}$ and $P_{d,t}$ are charging and discharging power limits respectively. Therefore, the following holds true for the battery charging/discharging status:

$$\omega_{c,t} + \omega_{d,t} = 1 \quad (11)$$

The multi-objective minimization function for demand response strategy is discussed in the following sections. The minimization function consists of the electricity cost, PAR reduction and discomfort minimization for consumers.

3.2.1 Electricity Cost

With regard to consumer participation in demand response program, electricity cost ($e_c(t)$) can be modelled according to [52]:

$$e_c(t) = \sum_{t=1}^{T} \sum_{i=1}^{N} P_{app,i} \cdot \lambda_t \cdot \omega_t \cdot \partial t \quad (12)$$

T is the total number of periods in scheduling cycle, t is the period number, ∂t is the length of each time period, N is the total number of schedulable appliances, i is appliance number, $P_{app,i}$ is the rated power of appliance i, λ_t is electricity price in period t, ω_t is the on/off status of appliance i in period t.

The schedulable appliances are used during periods of the day when the unit electricity price is comparatively lower.
(Note: Equation (12) applies to schedulable appliances only).

3.2.2 Peak-to-Average Ratio

The peak-to-average ratio (PAR) is considered in this paper because it affects the bonus incentive which the DR aggregator derives from the distribution utility. In other words, the smaller the value of PAR, the greater the bonus will be, and vice versa [53]. PAR is a stability index which balances conventional power generation cost with cost of maintaining renewable energy sources. Mathematically, it is defined as [54]:

$$\Pi\ (P,t) = \frac{peak\ load\ of\ smart\ grid}{average\ load\ of\ smart\ grid} = \frac{P_{max,t}}{\frac{1}{T}\sum_{t=1}^{T} P_t} \tag{13}$$

$P_{max,t}$ is the maximum power generated by the smart grid, P_t is the power generated within one time interval t, and T is total number of time intervals.

For this paper, the PAR is calculated on a daily basis for summer and winter days respectively. Therefore, T=24. The accrued bonus ($b(t)$) to the demand response (DR) aggregator from the utility with respect to PAR is an objective that needs to be maximized as [47]:

$$b(t) = \sigma \sum_{t=1}^{T} (c_{gen,conv,t} - c_{gen,DR,t}) \tag{14}$$

σ is the bonus coefficient, $c_{gen,conv,t}$ is the generation cost using conventional sources at time t, $c_{gen,DR,t}$ is generation cost with demand response at time t.

3.2.3 Discomfort

Demand side management programs result in some level of discomfort to the consumer as a result of the rescheduling of time-shiftable appliances. However, in order to encourage participation in demand response programs, the level of discomfort to the consumer must be kept within acceptable limits. In this paper, the level of consumer discomfort is modelled as:

$$D_{con,i}(P,t) = \begin{cases} 0 \le D \le 0.5 : \ P_{con,i,t} + P_{RES,i,t} \\ \quad 0.5 \le D \le 1 : \ P_{con,i,t} \end{cases} \tag{15}$$

$P_{con,i,t}$ is power consumed by consumer *i* with demand response, $P_{RES,i,t}$ is power consumed by consumer *i* with demand response and utilization of renewable energy sources , D is discomfort factor, $D_{con,i}(P,t)$ is discomfort factor of consumer *i* at time *t* given their energy consumption habits.

The discomfort factor is selected based on utilization of renewable energy sources by consumer. It is weighted such that a lower weighting (0 to 0.5) translates to a lower level of discomfort, and vice versa. In other words, the consumer is rewarded when renewable energy sources are utilized during peak pricing periods.

3.2.4 Uncertainty

The uncertainties considered in this paper are from the demand side of the power system. The solar PV module is subject to uncertainties based on the fluctuations in weather conditions, which can occur within a normal day in Johannesburg. Also, unpredictable user behaviour with regard to energy usage can introduce unplanned trends into the energy usage profile [45]. The exponential smoothing model for forecasting uncertainty is adopted in this paper [55]:

$$U_{\alpha,d} = \beta \overline{U}_{\alpha,d-1} + (1-\beta) U_{\alpha,d-1} \tag{16}$$

$\alpha = 1{,}2$ and represents the uncertainty of PV module and consumer behaviour respectively, β is smoothing factor of exponential smoothing model (0< β<1), $\overline{U}_{\alpha,d-1}$ is actual value of power output due to uncertainty of previous day, $U_{\alpha,d-1}$, $U_{\alpha,d}$ is forecasted uncertainty load values for previous and next day respectively.

The exponential smoothing model is a data pre-processing technique used for noise removal. It has been successfully applied in several forecasting and/or prediction techniques [61]-[62].

In order to represent the degree of uncertainty with respect to $U_{\alpha,d}$, $U_{\alpha,d-1}$ can be re-written as:

$$U_{\alpha,d-1} = \overline{U}_{\alpha,d-1}(1 + \rho_{\alpha}^{peak}\theta_{rand}) \tag{17}$$

ρ_{α}^{peak} is percentage representing degree of uncertainty of PV module and consumer behaviour respectively, θ_{rand} is random uniformly distributed number with interval [-1 1]. In particular, ρ_{1}^{peak}=5% and ρ_{2}^{peak}=8% (based on the assumption that consumer behaviour is marginally more erratic than weather uncertainty).

4 Improved Enhanced Differential Evolution (*i*EDE) Algorithm and Multi-objective Minimization Function

4.1 *i*EDE

Differential evolution (DE) selects the best-fitting solution(s) to a problem by continually testing candidates with a pre-determined standard (called a mutant vector) [60]. This is as a result of the role that the difference vector plays in guiding the mutant vector towards the global optimum. DE is effective in obtaining the most suitable solution to complex problems because of its rigorous competition strategy. This strategy allows even the mutant vector to be replaced when a better-performing candidate has been found. The steps involved in the DE selection strategy are: initialization, mutation, crossover and selection [26]. The mutation and crossover stages are vital to the performance of the DE algorithm; as such, several researchers have proposed improvements to these stages (called enhanced differential evolution (EDE)), in order to enhance its performance in demand side management [19]-[20], [25].

This paper proposes an improved enhanced DE algorithm (*i*EDE) using a two-archive approach for mutation and crossover (recombination). This approach is motivated by the following reasons:

1. The ever-increasing complexity of optimization problems (particularly with respect to the number of objectives) makes the challenge of balancing local exploitation with global exploration difficult [56]
2. The large dimension of the solution space makes it difficult for the mutation and recombination processes to produce fit offspring from genetically-compatible parents. In other words, fit parents do not always produce fit offspring. Furthermore, the large

dimension of solution space makes it difficult for compatible candidates to locate and mate with each other

With regard to the aforementioned, the two-archive approach is summarized by a 3-step flowchart in Fig. 4.

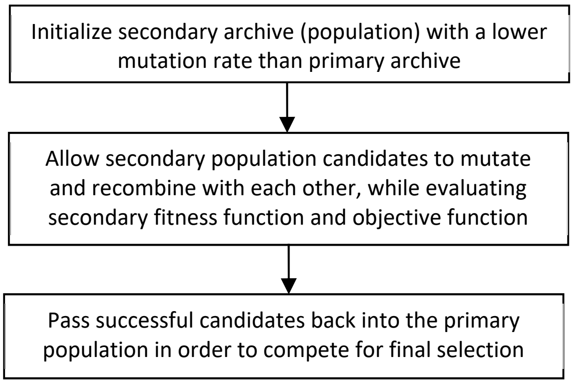

Fig. 4 Proposed two-archive DE

The primary archive adopts the evolutionary approach proposed in [20]. However, in order to prevent long computational time, the secondary archive has a size of $N_p/2$ (where N_p is the size of the primary archive). The crossover rate (CR) settings for the first three trial vectors for the primary (A_p) and secondary (A_s) archives are shown in Table 2.

Table 2 CR settings for DE/rand-to-best Strategy

Trial vectors	A_p	A_s
$xr_{1,G}$	0.3	0.2
$xr_{2,G}$	0.6	0.4
$xr_{3,G}$	0.9	0.7

The trial vector settings for the primary archive have been adopted from [19]. In this paper, we will focus on the dynamics between convergence and diversity within the secondary archive. The primary archive uses the conventional EDE [20]. The mutation vector M_i is obtained according to the following:

$$M_{i,t} = x_{r1,G} + F(x_{r2,G} - x_{r3,G}) \tag{18}$$

F is the scaling factor with an upper limit of 1.0. $x_{r1,G}$, $x_{r2,G}$ and $x_{r3,G}$ are randomly chosen vectors in a given generation. $x_{r2,G}$ and $x_{r3,G}$ are difference vectors.

With regard to the population size of the secondary archive relative to the primary archive:

$$N_s = \frac{N_p}{2} \tag{19}$$

N_s is the size of secondary archive, and N_p is size of primary archive

With regard to the secondary archive, the mutation and recombination process is set such that the phenotype of particles evolves at a slower rate. This strategy is adopted since the archive is populated by ‘unfit’ individuals considered to be weaker than those in the primary archive. In particular, phenotype modification is determined using [56]:

$$p_t = p_{t-1} + \omega_{r,t} \tag{20}$$

p_t represents the phenotype of a particle within N_s at time t. p_{t-1} is the phenotypic state of the particle at time $t-1$ since the state of the particle is considered in a stepwise manner. $\omega_{r,t}$ is a random, normally distributed number added to the phenotype at time t with mean $\eta = 0$ and standard deviation $\mu = \mu_s$.

The fitness function of a particle i within N_s at time t is denoted as $F(N_{s,i}, t)$ and determined according to:

$$F(N_{s,i}, t) = \frac{f(p_{i,t-1})}{\sum_{i=1}^{N_s} f(p_{s,t-1})} \tag{21}$$

$f(p_{i,t-1})$ is the fitness of phenotypic fitness of particle i and $\sum_{i=1}^{N_s} f(p_{s,t-1})$ is the overall fitness of particles within the secondary archive.

With regard to diversity of N_s, it is important to consider the richness and evenness of the population [56]. The richness describes the variety that exists within genotype and phenotype of the secondary population, while the evenness describes the spread among genotypical attributes of the population (for example, the distribution of fit alleles within particle genomes). In order to ensure a good tradeoff between these two important attributes, the following relation is used:

$$g_{opt,t+1} = (1-\varepsilon) g_{opt,t} + \varepsilon \frac{(1-m)\epsilon_s g_{opt,t} + m(1-g_{opt,t})}{\epsilon_s g_{opt,t} + (1-g_{opt,t})} + N_s \cdot \varepsilon \tag{22}$$

$g_{opt,t+1}$ represents the improved genotype of particles within N_s, ε is replacement rate of unfit particles in N_s, m is the mutation rate, ϵ_s is the selection pressure. The last term ($N_s \cdot \varepsilon$) is added to ensure that the final selection of fit individuals with respect to particle lifetime within N_s is as optimal as possible.

In order to address the problem of distant solutions, the approach proposed in [57] is adopted to group fit candidates together. For any two clusters a and b, the shortest Euclidean distance is determined, and both clusters are grouped together according to (22) and (23):

$$d_E(a, b) = \sqrt{\frac{2 n_a n_b \cdot \|\overline{\sigma_a} - \overline{\sigma_b}\|^2}{(n_a - n_b)}} \tag{23}$$

$d_E(a, b)$ is the distance between a and b, n_a and n_b are the number of candidates in cluster a and b respectively, $\cdot \|\overline{\sigma_a} - \overline{\sigma_b}\|^2$ is the Euclidean distance between $\overline{\sigma_a}$ and $\overline{\sigma_b}$. Consequently, minimum distance between clusters is obtained according to:

$$\eta_j^{cent} = \frac{\sum_{k=1}^{n} \vartheta_{k,j}^{cl}}{n} \tag{24}$$

η_j^{cent} represents the jth objective value of the centre of cluster η, $\vartheta_{k,j}^{cl}$ is the jth objective value of the kth candidate in cluster η, n is the total number of candidates in cluster η.

The termination criterion used in the simulations is limited to the number of generations (N_{gen}). For the primary archive, N_{gen}=1,000 and for the secondary archive, N_{gen}=500. The general parameter settings for the simulations are summarized in Table 3, while the details of the proposed *i*EDE algorithm are outlined in Algorithm 1.

Table 3 Parameter Settings for *i*EDE Algorithm, EDE, MOEA/DD and NSGAIII

Parameter	Setting
Mutation factor (F)*	[0 2]
Number of Feature Evaluations (FEs)	10,000
Number of simulation runs per case	10
Mutation rate	1/n
Crossover rate (adaptive)	0.2 – 1.0
Population size*	N_p=100, N_s=50
Selection strategy*	DE/rand-to-best/1
Number of generations*	$N_{gen,p}$=1,000, $N_{gen,s}$ =500
Number of dimensions	100
Upper and lower limits for initial population*	x_i^L, x_i^u=[0 1]
Scaling factor*	F= [0.2 0.8]

*The mutation factor, selection strategy, and scaling factor apply to EDE and *i*EDE only. However, with regard to the population size, 100 search particles have been selected for MOEA/DD and NSGAIII to ensure uniform test conditions. Real-valued crossover has been used for all selected algorithms. The number of generations has been set to 1,000 for MOEA/DD and NSGAIII as termination criterion. All other parameter settings have been uniformly set for selected evolutionary algorithms to ensure that simulation results can be compared.

Algorithm 1. Pseudocode for *i*EDE Algorithm

Start
1 Input EDE parameters: CR, F, x_i^L, x_i^U, N_p, N_s, MaxGen
2 Initialize primary archive population N_p
3 Mutate N_p according to Equation (18)
4 Evaluate fitness of random solutions according to Equation (21)
5 If crossover probability (p_c) and mutation probability (p_m) are satisfied:
6 Select solutions
Else
7 Initialize secondary archive population N_s
8 Mutate N_s with $x_{r1,G}$=0.2, $x_{r2,G}$=0.4, $x_{r3,G}$=0.7
9 Vary $x_{r1,G}$, $x_{r2,G}$ and $x_{r3,G}$ adaptively until fitness of candidates is satisfied according to Equation (21)
10 Crossover and recombine candidates according to p_c and p_m until termination condition is satisfied
11 Add selected solutions from N_s to N_p
12 Repeat steps 2 to 6

End

4.2 Multi-objective Minimization Function

The objective minimization function is formulated using Equations (4), (12), (14), (15) and (16) as:

$$\min F(t) = \Gamma(\mathrm{t}) + e_c(t) - b(t) + D_{con,i}(P,t) + U_{\alpha,d}(t) \quad (25)$$

Subject to:

$$V_{pv,t} = V_{occ,t} + V_{m,t} \quad (26)$$
$$\beta_{t,min} \leq \beta_{t+1} \leq \beta_{t,max} \quad (27)$$
$$\beta_{t+1} \geq \beta_{t_0,t} \quad (28)$$
$$P_{max,t} = P_{pv,t} + P_{pv,T} \quad (29)$$
$$e_{d,t,T} \leq P_{conv,T} \quad (30)$$
$$e_{c,t,T} \leq P_{conv,T} \quad (31)$$

With regard to constraints in Equation (26) – (31):
$V_{pv,t}$ is the total voltage supplied by the solar PV module at time t, $V_{occ,t}$ is the terminal voltage of the PV module on no load, $V_{m,t}$ is the voltage supplied to a load m at time t.
$\beta_{t,min}$ is the state-of-charge of the battery in discharged state, β_{t+1} is the state-of-charge during a specified period, $\beta_{t,max}$ is the state-of-charge of battery in fully charged state
$\beta_{t_0,t}$ is battery state-of-charge at an initial starting instant in time
$P_{max,t}$ is the maximum power supplied by PV module, $P_{pv,t}$ is the power supplied by PV module at time t, $P_{pv,T}$ is power supplied after maximum time slot is achieved
$e_{d,t,T}$ is the battery discharge rate at time t, $P_{conv,T}$ is the total power converted and stored in the battery, $e_{c,t,T}$ is the battery charging rate at time t

The minimization function has been modelled as a convex function. Also, the performance of the proposed iEDE algorithm is compared to three other algorithms: EDE, multi-objective evolutionary algorithm based on dominance and decomposition (MOEA/DD) and non-dominated sorting genetic algorithm III (NSGAIII). The performance metric being used is the inverted generational distance (IGD), as well as the computational time. IGD calculates the average least distance from each point within a set of reference points to each point within the set of non-dominated solutions [58]. The smaller the IGD value, the better the convergence and diversity of the final solution set will be. The IGD is obtained according to [59]:

$$I(\upsilon,\upsilon') = \frac{\sum_{a\epsilon\upsilon'} min_{b\epsilon\upsilon} d_E(a,b)}{|\upsilon'|} \quad (32)$$

υ represents the objective values of non-dominated solution set obtained by MOEA, υ' is the set of uniformly distributed reference points from Pareto optimal front, $d_E(a,b)$ is the Euclidean distance between a and b.

5 RESULTS AND DISCUSSION

The performance of the proposed iEDE algorithm is compared with EDE, MOEA/DD and NSGA III in Table 4. From the results obtained using IGD metric and computational time, it can be seen that iEDE performs better than the three other algorithms for 7 out of 10 simulation runs. 10 simulation runs were used because it was observed that IGD values for all algorithms did not vary significantly beyond this number of runs. The IGD performance metric is a measure of both convergence and diversity of the solution candidates; this means that compared to the three other evolutionary algorithms, *i*EDE can generate the best possible solutions to the MOP. With regard to computational time, *i*EDE outperforms the other algorithms in 50% of the total simulation runs. From these results, it is observed that the secondary archive of *i*EDE adds to the computing overhead of the algorithm. This is because greater demand is placed on the computer processor as a result of parallel population sorting. In this regard, it is seen that NSGA III performs almost as well as the proposed algorithm.

The daily energy consumption for the proposed smart home for summer and winter weekdays is shown in Fig. 5 and Fig. 6 (before and after optimization with *i*EDE respectively). The usage profile shows that energy consumption peaks between 06:00-09:00 and also between 19:00-22:00 daily for both seasons (Fig. 5). This pattern is the same for weekend days as well. From Fig. 6, it can be seen that optimized energy usage via information from DR aggregator results in a flattened profile. This is as a result of rescheduling of shiftable appliances from peak periods to off-peak periods (Table 5). The five shiftable appliances have been selected because they contribute significantly to the daily energy consumption of the proposed smart home. Also, they are appliances which are used during both summer and winter seasons. This optimized energy usage schedule improves energy savings, and consequently reduces daily electricity costs. In particular, optimized energy usage profile for peak periods results in energy savings of 33% and 22% (at 08:00) for summer and winter weekdays respectively; also savings of 17.6% and 16.7% (at 21:00) for summer and winter weekdays respectively.

Table 4 IGD values and Computational time for 10 runs with *i*EDE, EDE, MOEA/DD and NSGA III

	iEDE	EDE	MOEA/DD	NSGA III
IGD	**5.09e-03**	2.13e-02	1.49e-02	2.58e-01
	6.14e-02	**2.27e-03**	2.71e-03	3.14e-02
	1.27e-02	5.19e-01	3.93e-02	3.18e-02
	3.92e-01	6.14e-01	4.17e-01	4.26e-01
	4.59e-04	6.67e-03	5.50e-02	3.37e-03
	2.05e-02	**3.12e-03**	6.19e-03	4.58e-03
	3.19e-01	2.04e+01	4.03e-01	5.66e-01
	5.25e-02	2.03e-01	3.05e+00	6.97e-01
	4.73e-02	2.93e-01	**1.12e-01**	4.18e-01
	3.93e-01	**2.07e-02**	4.77e-01	4.31e-01
Computational time (secs)	6.05e+02	**3.06e+02**	4.58e+02	5.96e+02
	3.19e+02	6.19e+02	4.44e+02	3.57e+02
	4.67e+02	5.05e+02	5.65e+02	4.82e+02

	1.27e+02	**2.12e+01**	1.93e+02	2.58e+02
	5.63e+01	2.55e+02	3.01e+02	4.36e+02
	2.52e+03	3,33e+02	4.15e+02	**3.14e+02**
	3.35e+02	5.28e+02	3.81e+02	**4.89e+01**
	3.78e+02	4.18e+02	4.66e+02	3.95e+02
	5.59e+02	3.12e+02	3.97e+01	**3.28e+01**
	4.69e+02	6.86e+02	7.50e+03	3.16e+03

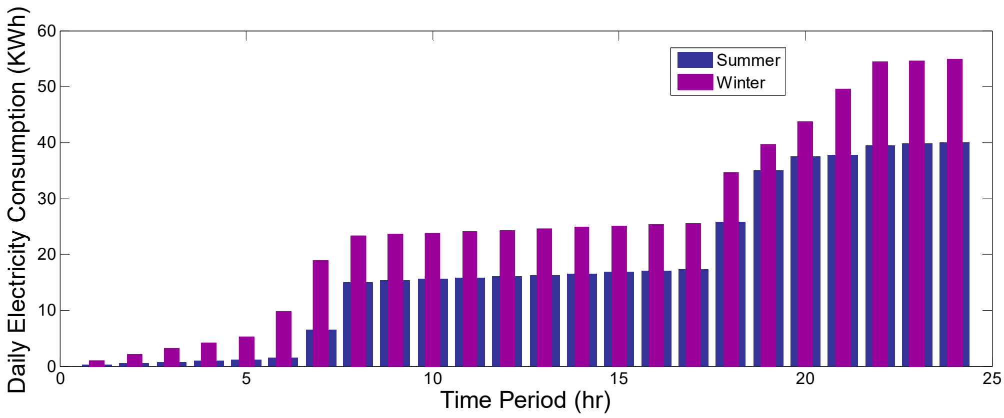

Fig. 5 Hourly Electricty consumption for proposed smart home for summer and winter weekdays (before optimization)

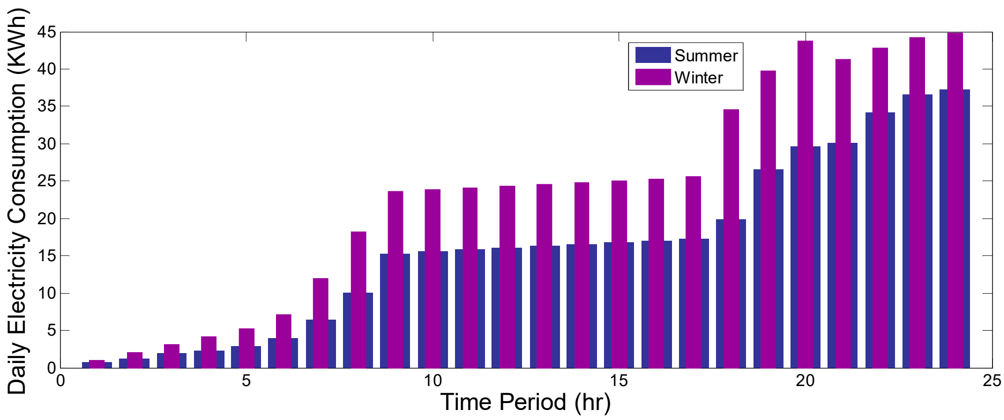

Fig. 6 Hourly Electricty consumption for proposed smart home for summer and winter weekdays (after optimization)

The level of discomfort to the consumer participating in DR program is estimated by considering the waiting time for both interruptable and uninterruptable appliances (Fig. 7). The performance of *i*EDE is compared to EDE for a selected peak hour (20:00-21:00 on weekday). From Fig. 7, it can be seen that *i*EDE yields a 41.7% time savings in hourly running time for uninterruptable appliances, and 39.3% time savings for interruptable appliances compared to EDE. This approach is based on the idea that waiting time is within the comfort level of the consumer. Therefore, the longer the waiting time, the greater the energy cost savings without sacrificing user comfort. Fig. 8 shows the PAR for consumers without DR, and those with DR using EDE and *i*EDE respectively. It can be seen that PAR for *i*EDE and EDE is 41.7% and 25% less respectively compared to a consumer without DR. Also, PAR for *i*EDE is 22% less than that for EDE.

User comfort is enhanced by minimizing the discomfort factor, *D* (Equation (15)). It is determined on an hourly basis for time-shiftable appliances. A comparison of appliance waiting time for sfiftable appliances is carried out based on renewable energy resource utilization relative to consumer demand response. Rooftop solar PV module was considered for the consumer with demand response. This comparison is based on the same peak hour for summer day considered in Fig. 7. In particular, we consider geyser, vacuum cleaner and electric iron as shiftable appliances. Comparison is made for EDE and *i*EDE respectively, since EDE outperforms NSGAIII and MOEAD/D. From the results shown in Table 6, it can be seen that operation of each one of the three shiftable appliances considered can be delayed for the specified period while still satisfying Equation (15). The *i*EDE algorithm yields longer waiting time for all three shiftable appliances which means it results in greater cost savings while considering user comfort for the selected peak hour.

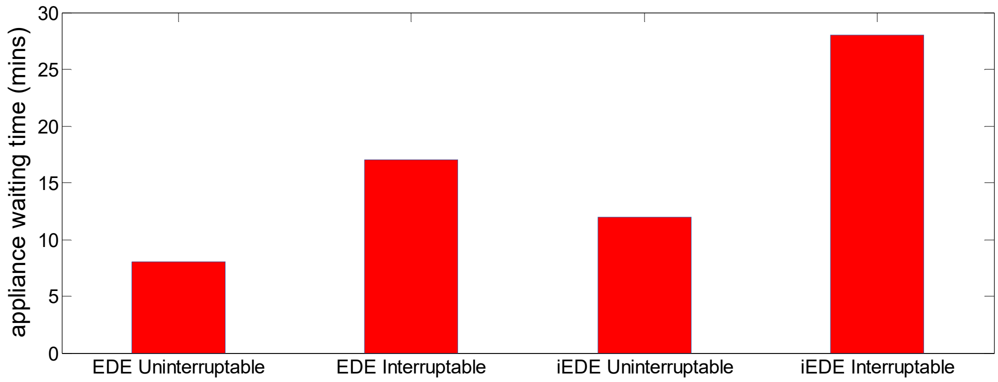

Fig. 7 Estimating user discomfort level using Appliance waiting time

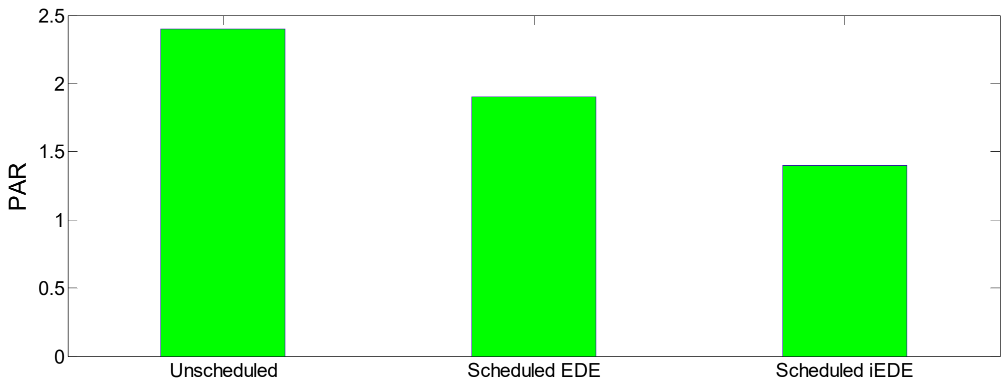

Fig. 8 PAR for consumer without DR, with DR using EDE and with DR using *i*EDE

Table 5 Optimized operating schedule for five shiftable appliances in proposed smart home

Appliance	Rating (KW)	Optimized schedule (Summer weekday)	Optimized schedule (Summer weekend day)	Optimized schedule (Winter weekday)	Optimized schedule (Winter weekend day)
Geyser	3.5	05:00-06:00, 18:00-19:00	06:00-07:00. 17:30-18:30	05:00-06:00, 18:00-19:00	06:00-07:00. 17:30-18:30
Vacuum cleaner	1.7	20:30-21:30	17:00-19:00	20:30-21:30	17:00-19:00
Electric iron	1.2	05:00-06:00. 20:30-21:30	05:30-06:30, 18:30-19:30	05:00-06:00. 20:30-21:30	05:30-06:30, 18:30-19:30
Miscellaneous loads	1.0	06:30-07:30, 18:00-19:30	14:00-18:00, 21:30-23:00	06:30-07:30, 18:00-19:30	14:00-18:00, 21:30-23:00
Dishwasher	1.0	06:45-07:45, 19:30-20:30	14:00-15:00, 21:30-22:30	06:45-07:45, 19:30-20:30	14:00-15:00, 21:30-22:30

Table 6 Comparison of Maximum Allowable Waiting Time for EDE and *i*EDE Based on Discomfort Factor, *D* for summer day peak hour (20:00-21:00)

Shiftable Appliance	Maximum Allowable Waiting Time (EDE)	Maximum Allowable Waiting Time (*i*EDE)
Geyser	15 mins	18 mins
Vacuum cleaner	21 mins	26 mins
Electric iron	17 mins	23 mins

6 CONCLUSION

This paper has discussed the implementation of demand response programs for electricity consumers using evolutionary algorithms. Specifically, an improved EDE (*i*EDE) algorithm using two population archives has been proposed for optimizing energy consumption parameters with the influence of demand response aggregator. In this paper, an instance of interaction of a single home energy management system with the demand response aggregator has been considered. This model can be extended to multiple users by considering parameter variations on the objective function based on different energy consumption requirements. It has been demonstrated that the two-archive approach improves the performance of EDE with regard to parameter optimization. It has also been shown that *i*EDE scales well with two other well-performing evolutionary algorithms (MOEA/DD and NSGA III). In particular, *i*EDE outperformed EDE, MOEA/DD and NSGA III with regard to convergence and diversity of the final solution set. The proposed algortihm also performed favourably in terms of computional time to obtain the optimal parameter settings for maximizing energy cost savings compared to the other considered algorithms. Specifically, energy cost savings is maximized by a minimization of the peak-to-average ratio between the demand response aggregator and the energy utility. In other words, a low value of peak-to-average ratio results in increased monetary bonus to the aggregator; this results in increased financial incentive being paid to consumers for reduced energy consumption. In terms of maximizing energy cost savings and user comfort, and minimizing PAR, it has been shown that *i*EDE achieves good performance for selected consumer case study.

With respect to the adaptability of the proposed model for multiple users, the renewable energy resource utilization coefficient (Equations (2), (3) and (4)) is proposed to handle cases which involve multiple households with different combination of renewable energy sources. The coefficient is obtained in such a way that it measures how much the consumer relies on renewable sources versus conventional power supply on a daily (hourly) basis. The research in this paper has focused on a single consumer; however, future research would examine the capability of *i*EDE to optimize the selected objectives with respect to reducing overall computational time for multiple consumers.

In summary, the following deductions can be made:

(1) Integrating alternative renewable energy sources using the proposed renewable energy source utilization coefficient (Equation 2) improves financial cost savings for the consumer. In other words, increasing the number of renewable energy sources increases compensation to demand response aggregator, and consequently to the consumer.
(2) Incorporating demand response aggregators into existing power systems will encourage judicious energy usage among consumers. This will benefit both energy utilities and demand response aggregators. Energy utilities will maximize usage of energy distribution infrastructure, while the demand response aggregators will maximize financial compensation from the utilities.
(3) Differential evolution is an effective evolutionary algorithm for optimizing parameters for the DR aggregator and the home energy management system. The proposed two-archive approach for mutation and recombination improves the performance of the earlier proposed enhanced differential evolution algorithm. In particular, the slower phenotypic modification rate adopted in the secondary archive was effective in improving performance. Therefore, evolutionary algorithms can play a vital role in improving demand response for both consumers and energy utility companies.

While the paper has highlighted the important role of DR aggregator in providing optimized energy scheduling for consumers, there is still a need to improve the performance of the proposed algorithm with regard to its computational demands. Therefore, future research will focus on how to improve the portability of the two-archive approach for mutation and recombination of candidate solutions. Also, the performance of the proposed aggregator has not been evaluated with the dynamics of the energy distribution utility. There is therefore the need to ascertain the robustness of the proposed system in the presence of energy supply system parameters.

ACKNOWLEDGEMENTS

This research is supported partially by South African National Research Foundation Grants (No. 112108 and 112142), and South African National Research Foundation Incentive Grant (No. 95687 and 114911), Eskom Tertiary Education Support Programme Grants (Y. Sun, Z. Wang), Research grant from URC of University of Johannesburg.

REFERENCES

[1] Z. M. Fadlullah and N. Kato, Evolution of Smart Grids, Springer International Publishing, Switzerland, 2015.
[2] R.L.Moen, “Solar energy management system”, Honeywell Inc. Energy Resource Center. 1979.
[3] H. Shareef, M. S. Ahmed, A. Mohamed and E. Al Hassan, "Review on Home Energy Management System Considering Demand Responses, Smart Technologies, and Intelligent Controllers," *IEEE Access,* vol. 6, pp. 24498-24509, 2018. . DOI: 10.1109/ACCESS.2018.2831917.
[4] Y. Liu, W. Wang and N. Ghadimi, "Electricity load forecasting by an improved forecast engine for building level consumers," *Energy,* vol. 139, pp. 18-30, Nov 15, 2017. Available: https://www.sciencedirect.com/science/article/pii/S0360544217313348. DOI: 10.1016/j.energy.2017.07.150.
[5] M. Mohammadi, F. Talebpour, E. Safaee, N. Ghadimi and O. Abedinia, "Small-Scale Building Load Forecast based on Hybrid Forecast Engine," *Neural Process Lett,* vol. 48, *(1),* pp. 329-351, Aug, 2018. . DOI: 10.1007/s11063-017-9723-2.
[6] P. Faria, J. Spinola and Z. Vale, "Aggregation and Remuneration of Electricity Consumers and Producers for the Definition of Demand-Response Programs," *Tii,* vol. 12, *(3),* pp. 952-961, Jun, 2016. Available: https://ieeexplore.ieee.org/document/7442137. DOI: 10.1109/TII.2016.2541542.
[7] S. K. Polaki, M. Reza and D. S. Roy, "A genetic algorithm for optimal power scheduling for residential energy management," in Jun 2015, pp. 2061-2065Available: https://ieeexplore.ieee.org/document/7165494. DOI: 10.1109/EEEIC.2015.7165494.
[8] N. G. Paterakis, A. Tascikaraoglu, O. Erdinc, A. G. Bakirtzis and J. P. S. Catalao, "Assessment of Demand-Response-Driven Load Pattern Elasticity Using a Combined Approach for Smart Households," *Tii,* vol. 12, *(4),* pp. 1529-1539, Aug, 2016. Available: https://ieeexplore.ieee.org/document/7500042. DOI: 10.1109/TII.2016.2585122.
[9] F. Y. Melhem, O. Grunder, Z. Hammoudan and N. Moubayed, "Optimal residential load scheduling model in smart grid environment," in Jun 2017, pp. 1-6Available: https://ieeexplore.ieee.org/document/7977436. DOI: 10.1109/EEEIC.2017.7977436.
[10] M. F. Shaaban, A. H. Osman and M. S. Hassan, "Day-ahead optimal scheduling for demand side management in smart grids," in Nov 2016, pp. 124-129Available: https://ieeexplore.ieee.org/document/7920240. DOI: 10.1109/EMS.2016.031.
[11] H. Leng, X. Li, J. Zhu, H. Tang, Z. Zhang and N. Ghadimi, "A new wind power prediction method based on ridgelet transforms, hybrid feature selection and closed-loop forecasting," *Advanced Engineering Informatics,* vol. 36, pp. 20-30, Apr, 2018. Available: https://www.sciencedirect.com/science/article/pii/S1474034617303154. DOI: 10.1016/j.aei.2018.02.006.
[12] O. Abedinia, N. Amjady and N. Ghadimi, "Solar energy forecasting based on hybrid neural network and improved metaheuristic algorithm," *Computational Intelligence,* vol. 34, *(1),* pp. 241-260, Feb, 2018. Available: https://onlinelibrary.wiley.com/doi/abs/10.1111/coin.12145. DOI: 10.1111/coin.12145.
[13] Yue Wang and D. Infield, "Optimal demand side response to real time price signal using electric vehicles," in 2015, pp. 6Available: http://digital-library.theiet.org/content/conferences/10.1049/cp.2015.0325. DOI: 10.1049/cp.2015.0325.
[14] S. S. Raghavan, "Impact of demand response on electric vehicle charging and day ahead market operations," in Feb 2016, pp. 1-7Available: https://ieeexplore.ieee.org/document/7459218. DOI: 10.1109/PECI.2016.7459218.

[15] Enxin Yao, P. Samadi, V. W. S. Wong and R. Schober, "Residential Demand Side Management Under High Penetration of Rooftop Photovoltaic Units," *Tsg,* vol. 7, *(3),* pp. 1597-1608, May, 2016. Available: https://ieeexplore.ieee.org/document/7254234. DOI: 10.1109/TSG.2015.2472523.
[16] N. Nikmehr and S. Najafi-Ravadanegh, "Optimal operation of distributed generations in micro-grids under uncertainties in load and renewable power generation using heuristic algorithm," *IET Renewable Power Generation,* vol. 9, *(8),* pp. 982-990, Nov, 2015. Available: http://digital-library.theiet.org/content/journals/10.1049/iet-rpg.2014.0357. DOI: 10.1049/iet-rpg.2014.0357
[17] D. Li, W. Chiu, H. Sun and H. V. Poor, "Multiobjective Optimization for Demand Side Management Program in Smart Grid," *Tii,* vol. 14, *(4),* pp. 1482-1490, Apr, 2018. Available: https://ieeexplore.ieee.org/document/8186194. DOI: 10.1109/TII.2017.2776104.
[18] S. L. Arun and M. P. Selvan, "Intelligent Residential Energy Management System for Dynamic Demand Response in Smart Buildings," *Jsyst,* vol. 12, *(2),* pp. 1329-1340, Jun, 2018. Available: https://ieeexplore.ieee.org/document/7829298. DOI: 10.1109/JSYST.2017.2647759.
[19] N. U. Rehman, N. Javaid and Z. A. Khan, "An enhanced differential evolution based energy management system for smart grids," in Mar 2017, pp. 132-137Available: https://ieeexplore.ieee.org/document/7929667. DOI: 10.1109/WAINA.2017.121.
[20] I. Fatima, N. Javaid, S. Shafiq, S. Asif, M. H. Rahim and S. Aslam, "Comparative study of meta-heuristic approaches towards utilization of home energy management: Comparative meta-heuristic approaches," in Mar 2018, pp. 1-6Available: https://ieeexplore.ieee.org/document/8346436. DOI: 10.1109/ICOMET.2018.8346436.
[21] Samadi, P., Wong, V.W. and Schober, R., 2016. Load scheduling and power trading in systems with high penetration of renewable energy resources. IEEE Transactions on Smart Grid, 7(4), pp.1802-1812.
[22] Javaid, N., Ullah, I., Akbar, M., Iqbal, Z., Khan, F.A., Alrajeh, N. and Alabed, M.S., 2017. An intelligent load management system with renewable energy integration for smart homes. IEEE Access, 5, pp.13587-13600.
[23] Khalid, A., Javaid, N., Guizani, M., Alhussein, M., Aurangzeb, K. and Ilahi, M., 2018. Towards dynamic coordination among home appliances using multi-objective energy optimization for demand side management in smart buildings. IEEE Access.
[24] Hussain, H.M., Javaid, N., Iqbal, S., Hasan, Q.U., Aurangzeb, K. and Alhussein, M., 2018. An Efficient Demand Side Management System with a New Optimized Home Energy Management Controller in Smart Grid. Energies, 11(1), p.190.
[25] S. Kazmi, N. Javaid, M. J. Mughal, M. Akbar, S. H. Ahmed and N. Alrajeh, "Towards optimization of metaheuristic algorithms for IoT enabled smart homes targeting balanced demand and supply of energy," *Access,* pp. 1, Oct 16, 2017. Available: https://ieeexplore.ieee.org/document/8070309. DOI: 10.1109/ACCESS.2017.2763624.
[26] A.E. Eiben and J.E. Smith, “Introduction to evolutionary computing,” Springer, 2nd Ed., 2015, pp. 25-41, 49-57.
[27] “Particle swarm optimization,” A. Lazinica (Ed.), In-Tech, 2009, pp. 1-10.
[28] J. Dreo, A. Petrowski, P.Siarry and E. Taillard, “Metaheuristics for hard optimization: methods and case studies,” Springer, 2006, pp. 75-92.
[29] S. Rahim, N. Javaid, A. Ahmad, S. A. Khan, Z. A. Khan, N. Alrajeh and U. Qasim, "Exploiting heuristic algorithms to efficiently utilize energy management controllers with renewable energy sources," *Energy & Buildings,* vol. 129, pp. 452-470, Oct 1, 2016. Available: https://www.sciencedirect.com/science/article/pii/S0378778816306867. DOI: 10.1016/j.enbuild.2016.08.008.
[30] M. Loesch, D. Hufnagel, S. Steuer, Tillman Faßnacht and Hartmut Schmeck, “Demand side management in smart buildings by intelligent scheduling of heat pumps,” *2014 IEEE International Conference on Intelligent Energy and Power Systems (IEPS)*, 2014, pp. 1-6.
[31] Y. Zhang, P. Zeng and C. Zang, “Optimization algorithm for home energy management system based on artificial bee colony in smart grid,” 5th Annual IEEE International Conference on Cyber Technology in Automation, Control and Intelligent Systems, June 2015, pp. 734-740.
[32] A. R. S. Vidal, L. A. A. Jacobs and L. S. Batista, "An evolutionary approach for the demand side management optimization in smart grid," in Dec 2014, pp. 1-7 Available: https://ieeexplore.ieee.org/document/7011561. DOI: 10.1109/CIASG.2014.7011561.

[33] Yimin Zhou, Guoqing Xu and Ming Chang, "Demand side management for EV charging/discharging behaviours with particle swarm optimization," in Jun 2014, pp. 3660-3664 Available: https://ieeexplore.ieee.org/document/7053325. DOI: 10.1109/WCICA.2014.7053325.
[34] Yimin Zhou and Guoqing Xu, "Demand side energy management with PSO and regulated electric vehicles behaviours," in Dec 2014, pp. 1-6 Available: https://ieeexplore.ieee.org/document/7066103. DOI: 10.1109/APPEEC.2014.7066103.
[35] M. M. Hossain, K. R. Zafreen, A. Rahman, M. A. Zamee and T. Aziz, "An effective algorithm for demand side management in smart grid for residential load," in Sep 2017, pp. 336-340 Available: https://ieeexplore.ieee.org/document/8255377. DOI: 10.1109/ICAEE.2017.8255377.
[36] M. Awais, N. Javaid, N. Shaheen, Z. Iqbal, G. Rehman, K. Muhammad and I. Ahmad, "An efficient genetic algorithm based demand side management scheme for smart grid," in Sep 2015, pp. 351-356 Available: https://ieeexplore.ieee.org/document/7350643. DOI: 10.1109/NBiS.2015.54.

[37] N. K. Paliwal, R. Mohanani, N. K. Singh and A. K. Singh, "Demand side energy management in hybrid microgrid system using heuristic techniques," in Mar 2016, pp. 1910-1915 Available: https://ieeexplore.ieee.org/document/7475058. DOI: 10.1109/ICIT.2016.7475058.
[38] S. K. Nayak, N. C. Sahoo and G. Panda, "Demand side management of residential loads in a smart grid using 2D particle swarm optimization technique," in Oct 2015, pp. 201-206 Available: https://ieeexplore.ieee.org/document/7438160. DOI: 10.1109/PCITC.2015.7438160.
[39] A. Khalid, N. Javaid, A. Mateen, B. Khalid, Z. A. Khan and U. Qasim, "Demand side management using hybrid bacterial foraging and genetic algorithm optimization techniques," in Jul 2016, pp. 494-502 Available: https://ieeexplore.ieee.org/document/7791933. DOI: 10.1109/CISIS.2016.128.
[40] A. Silva, J. Marinheiro, H. Lopes Cardoso and E. Oliveira, "Demand-side management in power grids: An ant colony optimization approach," in Oct 2015, pp. 300-306 Available: https://ieeexplore.ieee.org/document/7371387. DOI: 10.1109/CSE.2015.31.
[41] E. Galván-López, M. Schoenauer and C. Patsakis, "Design of an autonomous intelligent demand-side management system by using electric vehicles as mobile energy storage units by means of evolutionary algorithms," in Nov 9, 2015, pp. 106-115 Available: https://hal.inria.fr/hal-01254912. DOI: 10.5220/0005607401060115.
[42] Z. Garroussi, R. Ellaia, E. Talbi and J. Lucas, "Hybrid evolutionary algorithm for residential demand side management with a photovoltaic panel and a battery," in May 2017, pp. 4-10 Available: https://ieeexplore.ieee.org/document/8252952. DOI: 10.1109/ICCAIRO.2017.10.
[43] B. Lokeshgupta, A. Sadhukhan and S. Sivasubramani, "Multi-objective optimization for demand side management in a smart grid environment," in Dec 2017, pp. 200-205 Available: https://ieeexplore.ieee.org/document/8387293. DOI: 10.1109/ICPES.2017.8387293.
[44] T. Logenthiran, D. Srinivasan and Ei Phyu, "Particle swarm optimization for demand side management in smart grid," in Nov 2015, pp. 1-6 Available: https://ieeexplore.ieee.org/document/7386973. DOI: 10.1109/ISGT-Asia.2015.7386973.
[45] X. Yang, Y. Zhang, H. He, S. Ren and G. Weng, "Real-Time Demand Side Management for a Microgrid Considering Uncertainties," *Tsg,* pp. 1, Apr 9, 2018. Available: https://ieeexplore.ieee.org/document/8334652. DOI: 10.1109/TSG.2018.2825388.
[46] J. Corbett, K. Wardle and C. Chen, "Toward a sustainable modern electricity grid: The effects of smart metering and program investments on demand-side management performance in the US electricity sector 2009-2012," *Tem,* vol. 65, *(2),* pp. 252-263, May, 2018. Available: https://ieeexplore.ieee.org/document/8263195. DOI: 10.1109/TEM.2017.2785315.
[47] L. Gkatzikis, I. Koutsopoulos, and T. Salonidis, "The role of aggregators in smart grid demand response markets," IEEE J. Selected Areas in Communications, vol. 31, no. 7, pp. 1247–1257, July 2013.
[48] Climate: average monthly weather in Johannesburg, South Africa, Available: https://weather-and-climate.com/average-monthly-Rainfall-Temperature-Sunshine,johannesburg,South-Africa
[49] City power Johannesburg: Tariffs and Charges 2016/2017, Available: www.citypower.co.za/customers/Documents/City%20Power%20Tariffs%20Booklet_2016-2017.pdf
[50] M. Shakeri, M. Shayestegan, H. Abunima, S. M. S. Reza, M. Akhtaruzzaman, A. R. M. Alamoud, K. Sopian and N. Amin, "An intelligent system architecture in home energy management systems (HEMS) for efficient demand response in smart grid," *Energy & Buildings,* vol. 138, pp. 154-164, Mar 1, 2017. Available: https://www.sciencedirect.com/science/article/pii/S0378778816318369. DOI: 10.1016/j.enbuild.2016.12.026.
[51] O. Alrumayh and K. Bhattacharya, "Model predictive control based home energy management system in smartgrid", In Proceedings of the 2015 IEEE Electrical Power and Energy Conference, London, ON, Canada, 26–28 October 2015; pp. 152–157.

[52] X. Lu, K. Zhou, F. Chan and S. Yang, "Optimal scheduling of household appliances for smart home energy management considering demand response," *Nat Hazards,* vol. 88, *(3),* pp. 1639-1653, Sep, 2017. Available: https://search.proquest.com/docview/1924798795. DOI: 10.1007/s11069-017-2937-9.
[53] Yi Liu, Chau Yuen, Shisheng Huang, N. Ul Hassan, Xiumin Wang and Shengli Xie, "Peak-to-Average Ratio Constrained Demand-Side Management With Consumer's Preference in Residential Smart Grid," *Jstsp,* vol. 8, *(6),* pp. 1084-1097, Dec, 2014. Available: https://ieeexplore.ieee.org/document/6840951. DOI: 10.1109/JSTSP.2014.2332301.
[54] Y. Liu, C. Yuen, S. Huang, N. U. Hassan, X. Wang, and S. Xie, "Peak-to-average ratio constrained demand-side management with consumer's preference in residential smart grid," IEEE J. of Selected Topics in Signal Processing, vol. 8, no. 6, pp. 1084–1097, Dec 2014.
[55] S. H. Hong, M. Yu, and X. Huang, "A real-time demand response algorithm for heterogeneous devices in buildings and homes," Energy, vol. 80, pp. 123–132, 2015.
[56] I. Paenke, Y. Jin and J. Branke, "Balancing population- and individual-level adaptation in changing environments," *Adaptive Behavior,* 2009, pp.1-23.
[57] Y. Hua, Y. Jin and K. Hao, "A Clustering-Based Adaptive Evolutionary Algorithm for Multiobjective Optimization With Irregular Pareto Fronts," *Tcyb,* pp. 1-13, Jun 5, 2018. Available: https://ieeexplore.ieee.org/document/8372952. DOI: 10.1109/TCYB.2018.2834466.
[58] Y. Tian, X. Zhang, R. Cheng and Y. Jin, "A multi-objective evolutionary algorithm based on an enhanced inverted generational distance metric," 2016, pp. 1-9. DOI: 10.1109/CEC.2016.7748352
[59] A. Zhou, Y. Jin, Q. Zhang, B. Sendhoff, and E. Tsang, "Combining model-based and genetics-based offspring generation for multi-objective optimization using a convergence criterion," in *Proceedings of the 2006 Congress on Evolutionary Computation*, 2006, pp. 892–899.
[60] M. Leon and N. Xiong, "Investigation of Mutation Strategies in Differential Evolution for Solving Global Optimization Problems," in *Lecture Notes in Artificial Intelligence (LNAI 8467)*, Springer International Publishing, Switzerland, 2014, pp. 372-383.
[61] P. Lim and F. Wong, "Photovoltaic Power Predictions using Modified Adaptive Response Rate Exponential Smoothing Method," in *Proceedings of the 2016 IEEE International Conference on Sustainable Energy Technologies (ICSET)*, 2016.
[62] M. Abdurrahman, B. Irawan and R. Latuconsina, "Flood Forecasting using Holt-Winters Exponential Smoothing Method and Geographic Information System," in *Proceedings of 2017 International Conference on Control, Electronics, Renewable Energy and Communications (ICCEREC)*, 2017.